Smart Structures and Systems, *Vol. 15, No. 2 (2015) 489-503*
DOI: http://dx.doi.org/10.12989/sss.2015.15.2.489

Experimental validation of Kalman filter-based strain estimation in structures subjected to non-zero mean input

Rajendra P. Palanisamy[a], Soojin Cho[*], Hyunjun Kim[b] and Sung-Han Sim[c]

School of Urban and Environmental Engineering, Ulsan National Institute of Science and Technology (UNIST), Ulsan 689-798, Republic of Korea

(Received November 30, 2014, Revised January 8, 2015, Accepted January 13, 2015)

Abstract. Response estimation at unmeasured locations using the limited number of measurements is an attractive topic in the field of structural health monitoring (SHM). Because of increasing complexity and size of civil engineering structures, measuring all structural responses from the entire body is intractable for the SHM purpose; the response estimation can be an effective and practical alternative. This paper investigates a response estimation technique based on the Kalman state estimator to combine multi-sensor data under non-zero mean input excitations. The Kalman state estimator, constructed based on the finite element (FE) model of a structure, can efficiently fuse different types of data of acceleration, strain, and tilt responses, minimizing the intrinsic measurement noise. This study focuses on the effects of (a) FE model error and (b) combinations of multi-sensor data on the estimation accuracy in the case of non-zero mean input excitations. The FE model error is purposefully introduced for more realistic performance evaluation of the response estimation using the Kalman state estimator. In addition, four types of measurement combinations are explored in the response estimation: strain only, acceleration only, acceleration and strain, and acceleration and tilt. The performance of the response estimation approach is verified by numerical and experimental tests on a simply-supported beam, showing that it can successfully estimate strain responses at unmeasured locations with the highest performance in the combination of acceleration and tilt.

Keywords: response estimation; Kalman filter; data fusion; model error; non-zero mean input

1. Introduction

Structural health monitoring (SHM) is a process of monitoring the fitness of structures for timely maintenance to prevent catastrophic structural failures. To date, a wide variety of innovative SHM algorithms and applications have been studied as summarized by Li *et al*. (2014). In the field of civil, mechanical, and aerospace engineering, most of the structures are subjected to dynamic loads and gradual accumulation of fatigue damage may bring failure of structures (Palmgren 1924, Miner 1945, Shimokawa and Tanaka 1980, Fatemi and Yang 1998, Gresil *et al*. 2014, Wieghaus *et al*. 2014). Thus, monitoring fatigue is important for sustainable usage of the

*Corresponding author, Research Assistant Professor, E-mail: soojin@unist.ac.kr
[a] M.S. Student, E-mail: prasath@unist.ac.kr
[b] M.S. Student, E-mail: guswns3@unist.ac.kr
[c] Assistant Professor, E-mail: ssim@unist.ac.kr

http://www.techno-press.org/?journal=sss&subpage=8 ISSN: 1738-1584 (Print), 1738-1991 (Online)

structures. Accurate fatigue assessment is based on stress response time histories. Strain measurements are generally employed to obtain the stress time histories. In cases of complex civil structures like offshore structures subjected to complex loading requires strain measurements at several expected critical locations, it is practically and economically challenging to install strain gauges at all required locations. Thus, only limited physical sensor distribution is possible and a response estimation algorithm is necessary to obtain strain time history at other critical locations.

Response estimation at unmeasured locations from a small number of measurements has been attractive to the researchers who seek to overcome the limited instrumentation. Various efforts for response estimation has been made such as finite element model updating with modal expansion (Iliopoulos *et al*. 2014), natural input modal analysis (Hjelm *et al*. 2005), time varying auto-regressive model (Yazid *et al*. 2012), and the model-based Kalman state estimator. Among these efforts, the Kalman state estimator associated with the FE model has been known as an effective tool to estimate the unmeasured responses. Papadimitriou *et al*. (2009) used strain measurements in the numerical simulation to obtain strain in the entire body, which is subsequently utilized to estimate fatigue remaining life of the structural model. Smyth and Wu (2007) used the Kalman filter to fuse acceleration and displacement with different sampling rates to produce more accurate displacements. Based on the idea that multi-sensor data has the potential to improve the performance of response estimation (Park *et al*. 2013, Soman *et al*. 2014, Park *et al*. 2014, Cho *et al*. 2014), Jo and Spencer (2014) numerically verified that the combination of acceleration and strain in conjunction with the Kalman filter better estimates unmeasured strains compared to the sole use of acceleration or strain. Yet, the response estimation using the model-based Kalman filter with multi-sensor data has not been fully explored but limited to ideal numerical simulations with analytical FE models, the sole combination of acceleration and strain, and zero-mean random inputs.

This paper numerically and experimentally investigates the response estimation method using the Kalman filter with the limited number of multi-sensor data under the non-zero mean inputs. Because a number of full-scale civil engineering structures such as offshore structures are subjected to continuous fluctuating non-zero mean input forces, introducing the non-zero mean input excitation is considered to be more realistic. The performance of the estimation method is verified by numerical and experimental tests on a simply-supported beam. A model error is purposefully introduced in this work to consider possible inaccuracy of the model used to build the Kalman state estimator. In addition, four types of measurement combinations are used for the response estimation at the unmeasured locations: strain only, acceleration only, acceleration and strain, and acceleration and tilt. The combination of acceleration with strain or tilt (i.e., angular displacement) is considered for the data fusion, because acceleration captures the high frequency behavior of the structure in accuracy, while the strain and tilt can compensate the weakness in low frequency behavior and eventually increase the accuracy of estimation. For the four types of response combinations, the best combination is obtained by assessing the accuracies of the estimated responses.

2. Review of Kalman filter

Kalman filter was developed by Kalman (1960), which is a set of mathematical equations that provides an efficient computational (recursive) means to estimate the state of a process, in a way that minimizes the mean of the squared error. The Kalman state estimator based on Kalman filter is

employed here to estimate the unmeasured responses. The estimator requires three major inputs: system state, process noise, and measurement noise covariance. The limited physical measurements can be processed to obtain process and measurement noise covariance (Papadimitriou *et al*. 2009, Vinay *et al*. 2011, Lourens *et al*. 2012).

2.1 State space model

Equation of motion of a linear dynamic system is given as

$$\mathbf{M}\ddot{u}(t)+\bar{\mathbf{C}}\dot{u}(t)+\mathbf{K}u(t)=p(t) \tag{1}$$

where $u(t)$ is the displacement; its time derivatives $\dot{u}(t)$ and $\ddot{u}(t)$ are velocity and acceleration vectors, respectively; $\mathbf{M}$, $\bar{\mathbf{C}}$, and $\mathbf{K}$ are the mass, damping and stiffness matrices of the dynamic system, respectively; $p(t)$ is the input force vector.

Let $x(t)$ be the state vector given as

$$x(t)=\begin{Bmatrix}u(t)\\ \dot{u}(t)\end{Bmatrix} \tag{2}$$

Then, equation of motion is expressed in the state-space form as

$$\dot{x}(t)=\mathbf{A}x(t)+\mathbf{B}p(t)+\mathbf{G}w(t) \tag{3}$$

$$y(t)=\mathbf{C}x(t)+\mathbf{D}p(t)+\mathbf{H}w(t)+v(t) \tag{4}$$

where the matrices $\mathbf{C}$ and $\mathbf{D}$ in Eq. (4) are selected depending on the output of interest $y(t)$; process and measurement noises $w(t)$ and $v(t)$ are assumed to be stationary, mutually uncorrelated stochastic process following the normal probability distribution *w*; *N*(0, $\mathbf{Q}$) and $v:\ N(0,\mathbf{R})$, respectively; the matrices $\mathbf{G}$ and $\mathbf{H}$ are the coefficients of process noise. The system matrices $\mathbf{A}$ and $\mathbf{B}$ are defined as:

$$\mathbf{A}=\begin{bmatrix}\mathbf{0} & \mathbf{I}\\ -\mathbf{M}^{-1}\mathbf{K} & -\mathbf{M}^{-1}\bar{\mathbf{C}}\end{bmatrix} \tag{5}$$

$$\mathbf{B}=\begin{bmatrix}\mathbf{0}\\ \mathbf{M}^{-1}\end{bmatrix} \tag{6}$$

For example, if all the displacement and acceleration are to be estimated, the matrices $\mathbf{C}$ and $\mathbf{D}$ can be defined as

$$\mathbf{C}=\begin{bmatrix}\mathbf{I} & \mathbf{0}\\ -\mathbf{M}^{-1}\mathbf{K} & -\mathbf{M}^{-1}\bar{\mathbf{C}}\end{bmatrix} \tag{7}$$

$$\mathbf{D} = \begin{bmatrix} \mathbf{0} \\ \mathbf{M}^{-1} \end{bmatrix} \tag{8}$$

2.2 Kalman state estimator

A Kalman filter-based state estimator can be built to estimate the state $x(t)$.

$$\dot{\hat{x}} = \mathbf{A}\hat{x} + \mathbf{B}p + \mathbf{L}(z - \mathbf{C}\hat{x} - \mathbf{D}p) \tag{9}$$

where $\hat{x}$ is the estimated state of the state estimator, $\mathbf{L}$ is the Kalman gain, and z is the limited physical measurement. The Kalman gain $\mathbf{L}$ is defined as

$$\mathbf{L} = \left[P^{*}\mathbf{C}^{T} + \mathbf{G}\mathbf{Q}\mathbf{H}^{T} \right] \left[\mathbf{R} + \mathbf{H}\mathbf{Q}\mathbf{H}^{T} \right]^{-1} \tag{10}$$

where the error covariance P^{*} is obtained by minimizing the steady state error covariance.

$$P^{*} = \lim_{t \to \infty} E\left(\left\{ x - \hat{x} \right\} \left\{ x - \hat{x} \right\}^{T} \right) \tag{11}$$

3. Problem formulation

The formulation given in the previous section assumes zero-mean Gaussian random processes. Thus, the formulation is rebuilt in this section to incorporate the effect of nonzero mean input with multi-sensor data fusion. In this formulation, it is assumed that there is no input given to the system ($p(t) = 0$) rather the input is assumed to be only form the process noise $w(t)$. Thus, the coefficient of process noises $\mathbf{G}$ and $\mathbf{H}$ are replaced by $\mathbf{B}$ and $\mathbf{D}$ in Eqs. (3) and (4), respectively. Furthermore, process noise covariance $\mathbf{Q}$ is assumed as the covariance of input $p(t)$ to incorporate the effect of non-zero mean input. The unmeasured input covariance is obtained by processing the available limited response measurements (Papadimitriou *et al.* 2009). Following Eqs. (12) and (13) gives the modified state space model of the system.

$$\dot{x}(t) = \mathbf{A}x(t) + \mathbf{B}w(t) \tag{12}$$

$$y(t) = \mathbf{C}x(t) + \mathbf{D}w(t) + v(t) \tag{13}$$

With the modified state space model, a Kalman state estimator is constructed as

$$\dot{\hat{x}}(t) = \mathbf{A}\hat{x}(t) + \mathbf{L}(z - \mathbf{C}\hat{x}(t)) \tag{14}$$

$$y(t) = \mathbf{C}\hat{x}(t) \tag{15}$$

where z is the measured responses and Kalman gain $\mathbf{L}$ can be expressed as

$$\mathbf{L} = \left[P^{*}\mathbf{C}^{T} + \mathbf{BQD}^{T} \right] \left[\mathbf{R} + \mathbf{DQD}^{T} \right]^{-1} \tag{16}$$

The error covariance P^{*} minimizes the steady state error covariance as in Eq. (11). P^{*} is obtained by solving the algebraic Riccati equation which uses the modified noise covariance $\mathbf{Q}$. It is worthy to note that, for a given non-zero mean input, the output (i.e., response) is expected to be non-zero mean signal that may include multiple steady state and transition stages in time domain. To estimate such a complex response, P^{*} in Eq. (16) should minimize the steady state error covariance at all the stages in the response. The modified process noise $\mathbf{Q}$ enables the minimization, which enables the formulation to deal with the non-zero mean input and responses properly.

From Eq. (14), it can be inferred that value of filter gain $\mathbf{L}$ determines the priority between model and measurements in response estimation. From Eq. (16) for a given model (**A**, **B**, **C**, and **D**) and process noise $\mathbf{Q}$, the filter gain $\mathbf{L}$ is increased when the measurement noise covariance $\mathbf{R}$ decreases and vice versa. Thus estimation using sensors with lower noise level will depend more on measured responses than the given model and vice versa for sensors with higher noise floor. So using sensors with lower noise floor gives better estimation in situations where available numerical model is not accurate.

Here in this study, various sensors such as accelerometers, strain gauges, and tilt sensors are employed to investigate their characteristics and effects on the estimation performance depending on their noise levels and frequency ranges. In practice, strain gauges are considered to have a higher noise floor compared to accelerometers and tilt sensors. Strain gauges are sensitive to electrical noises and local defects in the structure. Acceleration being a poor low frequency observer, the quasi-static trend of non-zero mean responses is generally difficult to capture in comparison to tilt and strain gauges. Tilt sensors and strain gauges are poor high frequency observer compared to accelerometer. Because all three sensors are not perfect in all aspects, various combinations of sensors need to be investigated to maximize the accuracy of estimation under given erroneous model and the non-zero mean input condition.

4. Numerical simulation

In this section, a numerical model of a simply supported beam is employed to estimate strain responses from limited measurements using the modified Kalman state estimator.

4.1 Numerical model

A numerical simply-supported beam model was developed using MATLAB. The beam is composed of twenty Euler-Bernoulli beam elements each of which has the length of 0.1 m as shown in Fig. 1. The element has a rectangular cross-section of 1 cm thickness and 10 cm width. The Young's modulus and density of the material were selected as 206 GPa and 7580 kg/m^3 respectively. To analyze the effect of model error on the estimation accuracy, another numerical model is prepared with slight perturbation from the actual model. Perturbation in the new model is introduced by changing the elastic modulus and moment of inertia. Fig. 2 shows the comparison of frequency response functions (FRFs) from the simulation model and a model used in the Kalman

state estimator, where natural frequencies of both the model are considerably different.

The originally developed numerical model was used in MATLAB Simulink to simulate the acceleration, strain and angular displacement responses of the beam under a non-zero mean input shown in Fig. 3 applied at node 18. These responses sampled at 853 Hz with elliptic AA filter were used as reference response. The accelerations, strains, and tilt from a few selected nodes were contaminated by white noise. Accelerations and tilt are contaminate by 2% noise in root mean square (RMS), while the strains are contaminated by 10% noise in RMS based on the experience of higher noise on the actual strain measurement.

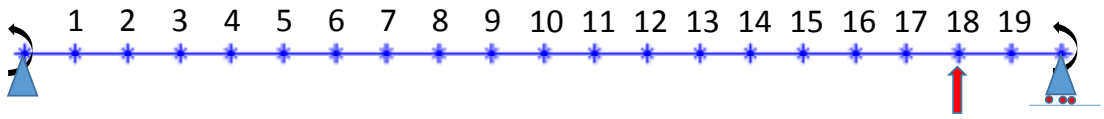

Fig. 1 Simply supported beam model

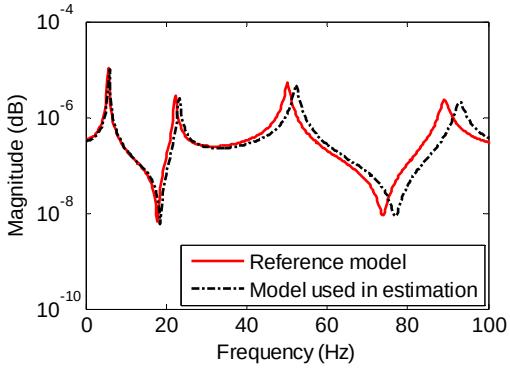

Fig. 2 Comparison of FRFs between reference and perturbed models

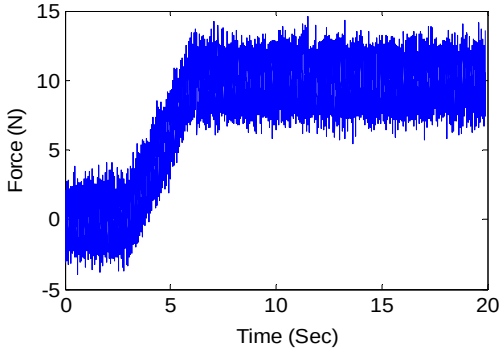

Fig. 3 Non-zero mean input excitation

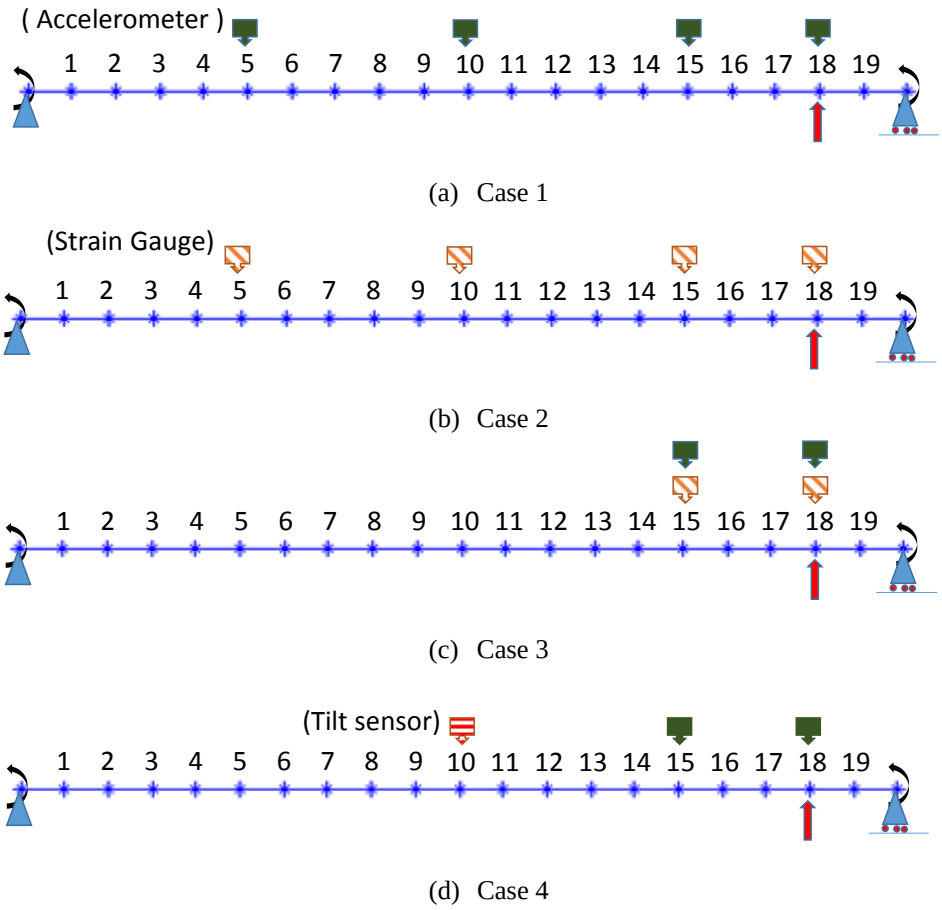

Fig. 4 Four measurement cases

4.2 Simulation cases

To verify the estimation performance, four types of measurements are considered as shown in Fig. 4. Cases 1 and 2 use strains and accelerations at nodes 5, 10, 15, and 18, respectively. Case 3 uses both accelerations and strains at nodes 15 and 18, and Case 4 uses two accelerations at nodes 15 and 18 and one tilt at node 10. Node 12 is the unmeasured location whose strain is to be estimated.

Fig. 5 and 6 show the estimated strain at node 12 in the time and frequency domains, respectively. Fig. 5 shows the estimated strain responses that have non-zero mean in more or less accuracy, except the Case 2 produces the zero-mean one whose quasi-static trend is unidentified. The result is consistent with the fact that given acceleration in the simulation does not contain the quasi-static behavior of the measured structure. Fig. 5 also shows that the multi-sensor cases (i.e., Cases 3 and 4) can better estimate the strain than the sole use of responses (i.e., Cases 1 and 2). Further comparing the multi-sensor data cases to each other, the combination of acceleration and

tilt resulted in more accurate estimation than the combination of acceleration with strain. Eq. (16) infers that the Kalman gain gives priority to measurement (i.e., tilt) combined with acceleration than response predicted from the model, when the measurements are less contaminated. Thus, Case 4 whose measurement has lower noise is less affected by the model error in the estimation than the other cases, as shown in Fig. 5.

The accuracy that is visually assessed in time domain as shown in Fig. 5 is investigated in frequency domain (see Fig. 6). For all measurement cases, four peak frequencies under 100 Hz (i.e., 5.8, 23.3, 52.1, and 92.9 Hz) are exactly estimated despite the model used for the Kalman state estimator is inexact. This shows that the Kalman filter-based estimation method has the robustness to the model error that is compensated due to using the measurements. The discrepancy is, however, observed in the anti-resonant frequency regions. In Fig. 6(b), Case 2 that uses only acceleration data has poor agreement with exact strain in the low frequency region under the first peak frequency, which reveals the failure in capturing the quasi-static trend in the strain. Whereas Case 1 (see Fig. 6(a)) has comparatively good agreement near 0 Hz, it has a higher noise floor compared to the reference. Comparing to Cases3 and 4 (see Figs. 6(c) and 6(d)), Case 4 that uses two accelerations with one tilt shows better agreement in both high and low frequency regions than Case 3 that uses two accelerations with two strains.

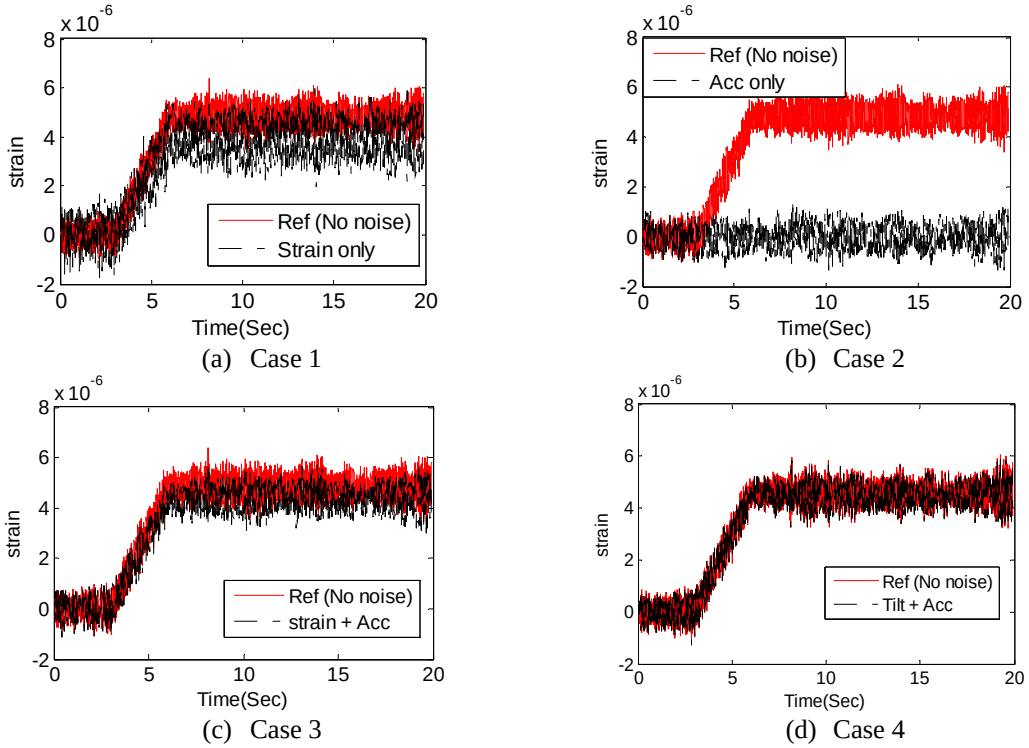

Fig. 5 Estimated and reference strain responses in time domain at node 12

To investigate the consistency of the response estimation method based on the Kalman filter, the strain responses were estimated for all locations. Instead of showing all the estimated responses compared with the exact ones, root mean square errors (RMSEs) between reference and estimated strains were calculated as:

$$Error = \frac{\sqrt{\sum\left(\varepsilon_{est} - \varepsilon_{ref}\right)^2}}{\sqrt{\sum\left(\varepsilon_{ref}\right)^2}} \tag{17}$$

where ε_{ref} is the reference strain and ε_{est} is the estimated strain.

Fig. 7 shows the RMSEs calculated for all nodes. Note that the RMSEs of Case 2 were quite large compared to the others due to inaccurate estimation of quasi-static strain component, and thus they were not plotted together. As to Case 1, the RMSEs are not consistent for all nodes and higher than those from Case 3 and Case 4, because during Kalman estimation of Case 1 a higher priority is given to erroneous model then the measurements due to higher noise floor. Case 4 has lower error for all nodes because the tilt contains lower level of noise than the strain used in Cases 1 and 3.

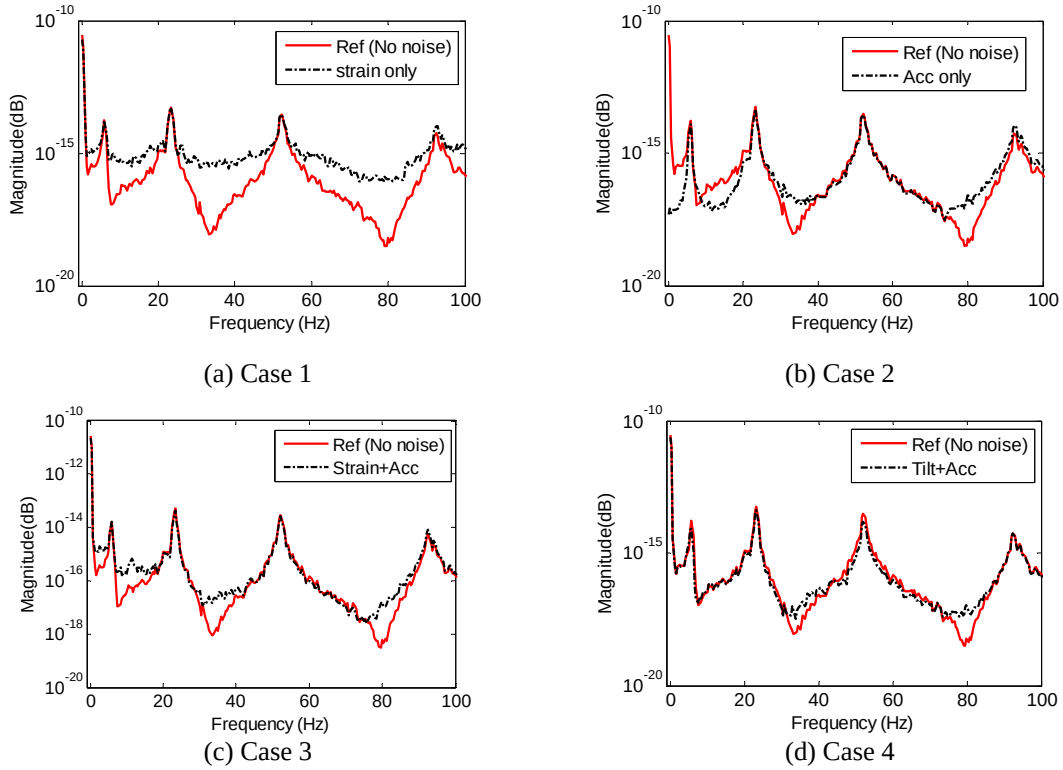

(a) Case 1 (b) Case 2

(c) Case 3 (d) Case 4

Fig. 6 Estimated and reference strain responses in frequency domain at node 12

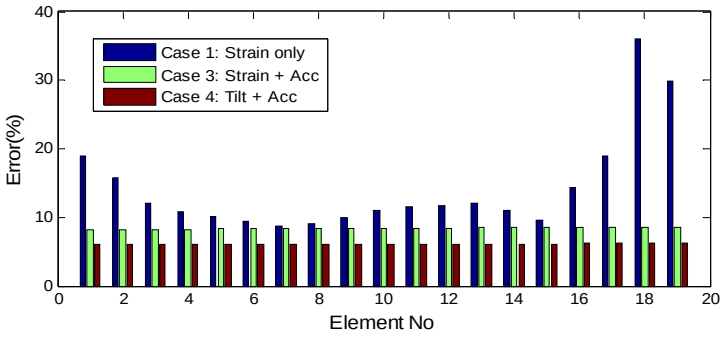

Fig. 7 Error of estimated strains at all nodes

5. Experimental validation

The section describes the laboratory-scale experiment for response estimation that is designed to replicate the numerical simulation.

5.1 Experimental setup

Fig. 8 shows the test beam whose length, width, and thickness are 2 m, 10 cm, and 1 cm, respectively. The Young's modulus and density of the beam are 206 GPa and 7860 kg/m^3, respectively. Since the test beam resembles the numerical beam in Fig. 1, the node number is assigned for every 0.1 m as Fig. 1. The test beam was excited with a non-zero mean force similar to Fig. 3 made by a shaker installed at node 18 (i.e., 0.2 m apart from the right support).

Four different experimental cases are performed and sensor deployment in each case is similar as in section 4.2. All the responses were sampled at 5 KHz using National Instruments data acquisition system (DAQ). Input voltage generated form DAQ was amplified using an amplifier and supplied to the shaker, and the responses from strain gauges, accelerometers and a tilt sensor were obtained simultaneously using the DAQ. Fig. 9 shows the difference between the FRFs from the experiment and the numerical model. The disagreement of the FRFs clearly shows the eligibility of inaccurate numerical model used in response estimation.

5.2 Estimation results

Fig. 10 shows the estimated strain responses according to four measurement cases compared to the measured strain at unmeasured node 12. Similar to the numerical simulation, all Cases estimated the strain response at the unmeasured node with somewhat accuracy, except Case 2.

Case 2 (see Fig. 10(b)) shows the inability of acceleration data to estimate the gradually increasing strain response. Case 1 (see Fig. 10(a)) resulted in the estimated strain with high noise level, while the multi-metric cases (i.e., Case 3 and Case 4) have lower noise levels (see Figs. 10(c) and 10(d)). Among the multi-metric cases, Case 3 could not estimate exact quasi-static response, while Case 4 resulted in the estimated strain with better agreement to the measured strain due to lower noise level of the tilt sensor than the strain gauges in practice.

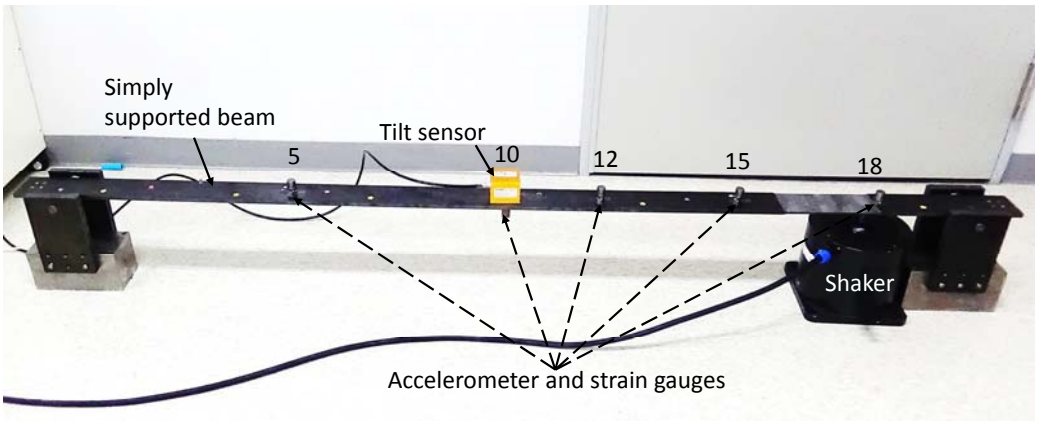

Fig. 8 Experimental beam structure with sensors and an actuator

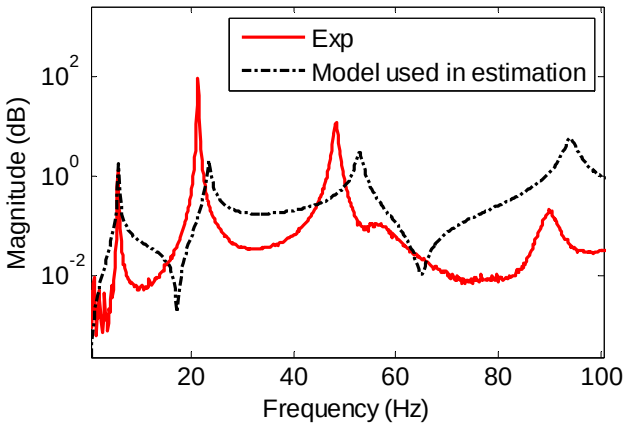

Fig. 9 Comparison of FRFs from experiment and numerical model

Fig. 11 is the comparison of estimated responses in the frequency domain. Note that the peak at 60 Hz in the measured strain is from the electrical noise around the laboratory where the experiment was carried out. First, unlike the reference strain used in the numerical simulation, the measured strain to be used as a reference contains high level of noise represented by flatness at the anti-resonant regions. This is the evidence why the strain was contaminated by higher level of noises than the other responses in the numerical simulation. Fig. 11(b) clearly shows that Case 2 has poor agreement in the low frequency region (near 0 Hz) related to quasi-static component of strain compared to other methods. Figs. 11(a), 11(c) and 11(d) show reasonable agreement of resonant peaks at 6.4, 22.6, 50.0, and 88.8 Hz, while there are some differences in the anti-resonant frequency regions. Among the results, Case 4 (see Fig. 11(d)) has the lowest level of noises at anti-resonant regions.

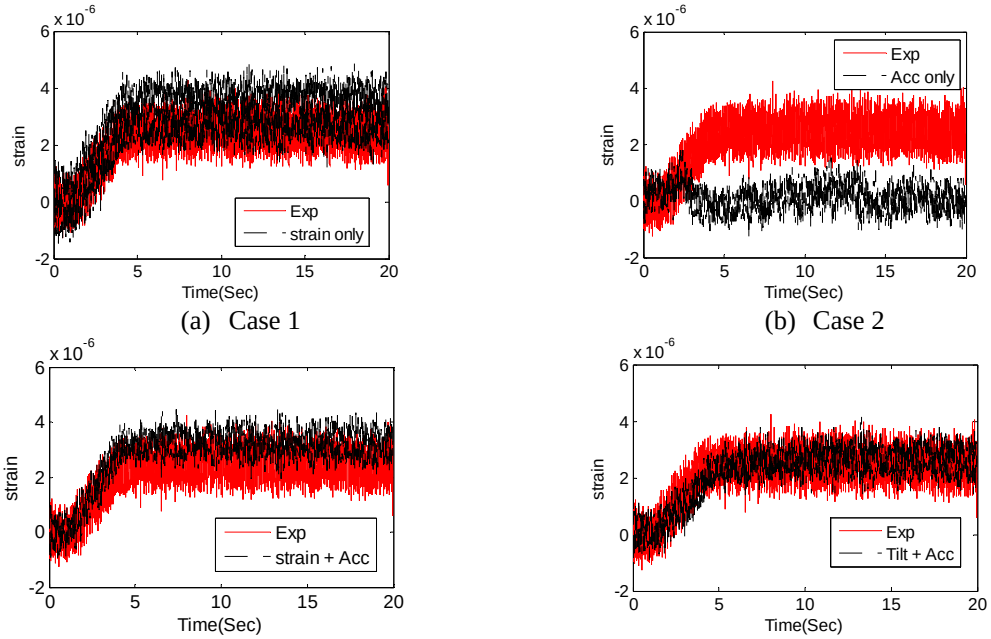

(a) Case 1 (b) Case 2

(c) Case 3 (d) Case 4

Fig. 10 Estimated and measured strain responses in time domain at node 12

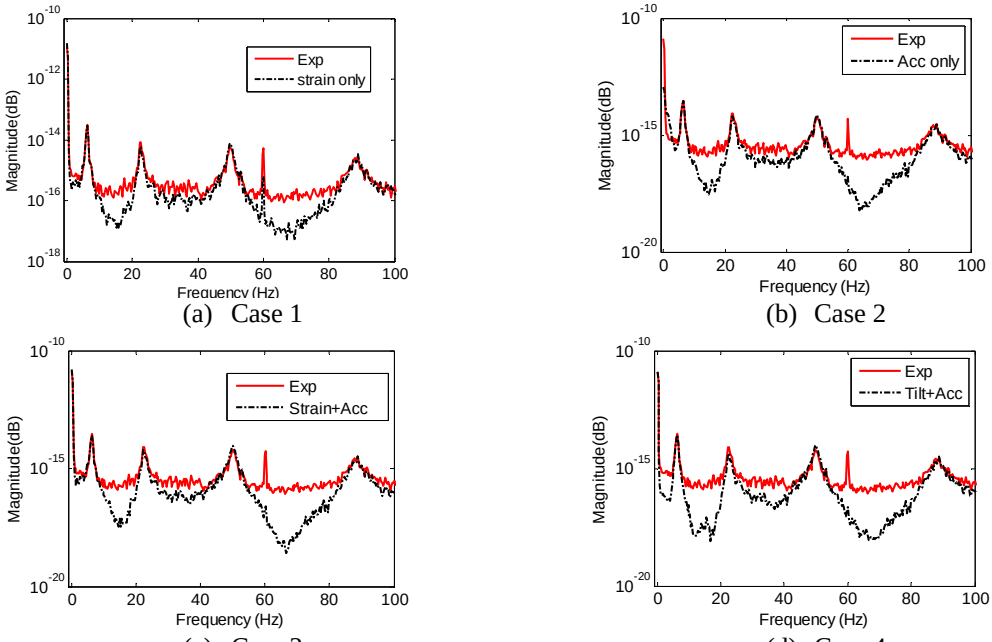

(a) Case 1 (b) Case 2

(c) Case 3 (d) Case 4

Fig. 11 Estimated and measured strain responses in frequency domain at node 12

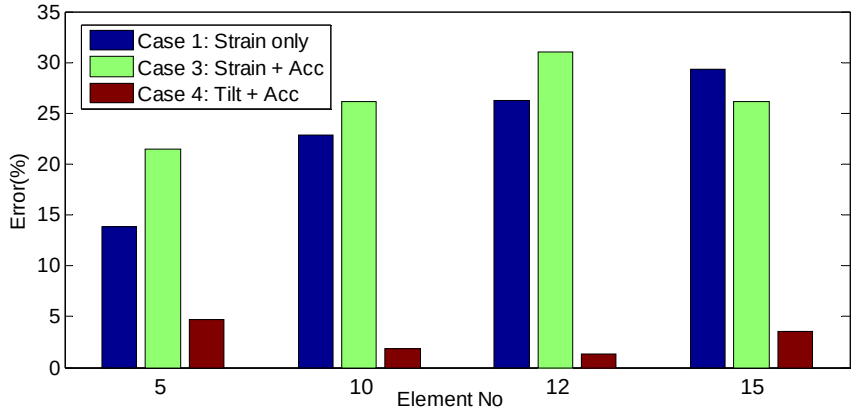

Fig. 12 Error in estimated strain

Fig. 12 shows the RMSEs between estimated and selected measurement strains. Note that the RMSEs of Case 2 are much larger than the others due to inaccurate quasi-static strain components, and thus they are not plotted together. Similar to Fig. 7, RMSEs from the numerical simulation, Case 4 showed smallest RMSEs less than 5%. Cases 1 and 3 are influenced by model error and noisy strain measurement, and thus higher RMSEs are estimated. Note that the RMSEs of Case 3 is slightly larger than those of Case 1 at several elements unlike the RMSEs of the numerical simulation shown in Fig. 7, because the reference strain used for comparison contains measurement noise in the experiment.

6. Conclusions

A response estimation technique based on Kalman state estimator has been redesigned to estimate strain responses at the unmeasured locations from a few measurements that are subjected to non-zero mean inputs. The Kalman state estimator has been modified by assuming the noise covariance as the variance of inputs to consider the non-zero mean inputs. Strain response estimation has been validated numerically and experimentally on a simply-supported beam using four different measurement cases. The result can be summarized as:

- The redesigned Kalman state estimator has successfully estimated the strain responses at the unmeasured locations excited by the non-zero mean inputs in the numerical and experimental validation tests, even with the erroneous model used in the Kalman state estimator.
- The acceleration has been figured out to be improper to estimate the quasi-static trend of non-zero mean strain response excited by the non-zero mean input due to lack of accuracy in low frequency measurement near 0 Hz.
- The multi-metric cases have produced the estimated response at the unmeasured locations with higher accuracy than the single-metric cases.

- Usage of strains that generally has higher noise level than acceleration or tilt has resulted in the estimated strain with higher level of noise.
- The combination of acceleration with tilt has been found best to estimate the response at the unmeasured locations with available erroneous model.

Acknowledgments

The research described in this paper was financially supported by the Ministry of Oceans and Fisheries, Korea (20110171). This research was a part of the project titled "Development of active-controlled tidal stream generation technology."

References

Bavdekar, V.A., Anjali, P.D. and Sachin, C.P. (2011), "Identification of process and measurement noise covariance for state and parameter estimation using Extended Kalman Filter", *J. Process Contr.*, **21**(4), 585-601.

Cho, S., Sim, S.-H., Park, J.W. and Lee, J. (2014), "Extension of indirect displacement estimation method using acceleration and strain to various types of beam structures", *Smart Struct. Syst.*, **14**(4), 699-718.

Gresil, M., Yu, L., Shen, Y. and Giurgiutiu, V. (2013), "Predictive model of fatigue crack detection in thick bridge steel structures with piezoelectric wafer active sensors", *Smart Struct. Syst.*, **12**(2), 97-119.

Fatemi, A. and Yang, L. (1998), "Cumulative fatigue damage and life prediction theories: a survey of the state of the art for homogeneous materials", *Int. J. Fatigue.*, **20**(1), 9-34.

Hjelm, H.P., Brincker, R., Graugaard-Jensen, J. and Munch, K. (2005), "Determination of stress histories in structures by natural input modal analysis", *Proceedings of the 23rd Conference and Exposition on Structural Dynamics (IMACXXIII)*, Orlando, Florida, USA, February.

Iliopoulos, A.N., Devriendt, C., Iliopoulos, S.N. and Van Hemelrijck, D. (2014), "Continuous fatigue assessment of offshore wind turbines using a stress prediction technique", *Proc. of SPIE, Health Monitoring of Structural and Biological Systems 2014*,Vol. 9064 90640S-1,San Diego, California, USA, March.

Jo, H. (2013), *Multi-scale structural health monitoring using wireless smart sensors*, PhD dissertation, University of Illinois at Urbana-Champaign.

Jo, H., and Spencer, B.F. (2014), "Multi-Metric model based structure health monitoring", *Proc. of SPIE, Sensors and Smart Structures Technologies for Civil, Mechanical, and Aerospace Systems 2014*, San Diego, California, USA, March.

Kalman, R.E. (1960), "A new approach to linear filtering and prediction problem", *J. Basic Engg.*, **82**(1), 35-45.

Li, H.N., Yi, T.H., Ren, L., Li, D.S. and Huo, L.S. (2014), "Reviews on innovations and applications in structural health monitoring for infrastructures", *Struct. Monit. Maint.*, **1**(1), 1-45.

Lourens, E., Papadimitriou, C., Gillijns, S., Reynders, E., Roeck, G.D. and Lombaert, G. (2012), "Joint input-response estimation for structural systems based on reduced-order models and vibration data from a limited number of sensors", *Mech. Syst. Signal Pr.*, **29**, 310-327.

Miner, M.A. (1945), "Cumulative damage in fatigue", *J. Appl. Mech. - T ASME*, **12**(3), 159-164.

Palmgren, A. (1924), "Die Lebensdauer von Kugallagern," *VDI-Zeitschrift.*, **68**(14), 339-341.

Papadimitriou, C., Fritzen, C.P., Kraemer, P. and Ntotsios, E. (2009), "Fatigue lifetime estimation in structures using ambient vibration measurements", *Proceedings of the ECCOMAS Thematic Conference on Computational Methods in Structural Dynamics and Earthquake Engineering*, Rhodes, Greece, June.

Papadimitriou, C., Fritzen, C.P., Kraemer, P. and Ntotsios, E. (2010), "Fatigue predictions in entire body of

metallic structures from a limited number of vibration sensors using Kalman filtering", *Struct. Control Health Monit.*, **18**(5), 554-573.

Park, J.W., Sim, S.-H., and Jung, H.J. (2013), "Displacement estimation using multimetric data fusion", *IEEE T. Mech. - ASME.*, **18**(6), 1675-1682.

Park, J.W., Sim, S.-H. and Jung, H.J. (2014), "Wireless displacement sensing system for bridges using multi-sensor fusion", *Smart Mater. Struct.*, **23**(4), 045022.

Shimokawa, T. and Tanaka S. (1980), "A statistical consideration of Miner's rule", *Int. J. Fatigue.*, **2**(4), 165-170.

Smyth, A. and Wu, M. (2007), "Multi-rate Kalman filtering for the data fusion of displacement and acceleration response measurements in dynamic system monitoring", *Mech. Syst. Signal Pr.*, **21**(2), 706-723.

Soman, R.N., Onoufriou, T., Kyriakides, M.A., Votsis, R.A. and Chrysostomou, C.Z. (2014), "Multi-type, multi-sensor placement optimization for structural health monitoring of long span bridges", *Smart Struct. Syst.*, **14**(1), 55-70.

Wieghaus, K.T., Hurlebaus, S. and Mander, J.B. (2014), "Effectiveness of strake installation for traffic signal structure fatigue mitigation", *Struct Monit. Maint.*, **1**(4), 393-409.

Yazid, E., Mohd, S.L., and Setyamartan, P. (2012),"Time-varying spectrum estimation of offshore structure response based on a time-varying autoregressive model", *J. Appl. Sci.*, **12**(23), 2383-2389.

Zhou, Y.E. (2006), "Assessment of bridge remaining fatigue life through field strain measurement", *J. Bridge Eng. - ASCE.*, **11**(6), 737-744.